ChemComm

COMMUNICATION

A scalable synthesis of pH-responsive polyacid nanogels: Injectable gel-forming hydrogel nanoparticles with a bright future

Received 00th January 20xx,
Accepted 00th January 20xx

DOI: 10.1039/x0xx00000x

www.rsc.org/

Amir H. Milani[a],*, Jennifer M. Saunders[a], Nam Trong Nguyen[a], Liam P. D. Ratcliffe[b] Steven P. Armes[b] Daman J. Adlam[c], Anthony J. Freemont[d], Judith A. Hoyland[c,d] and Brian R. Saunders[a],*

We report the first examples of pH-responsive polyacid nanogels with a swollen size less than 100 nm prepared by a scalable synthesis. Functionalisation of the nanogels was demonstrated using glycidyl methacrylate and the injectable dispersions formed transparent physical gels at physiological pH. The latter were mixed with polymer dots and covalently interlinked to give ductile near-infrared (NIR) hydrogels with potential application for imaging and soft tissue repair.

A nanogel is a crosslinked polymer nanoparticle which swells to a size less than 100 nm[1] in a good solvent or when the pH is greater (less) than the pK_a of the constituent polyacid (polybase) polymer. Nanogels have a high surface area for functionalisation[2], fast response times to environmental stimulus[3], enhanced circulation times in vivo and negligible scattering of light. These favourable properties have resulted in their study for imaging agents[4], paints[5], pastes[6], diagnostic systems[7] and delivery, especially for ocular delivery[3]. Although there have been a number of studies that have reported pH-responsive nanogels[1-4, 8-12] the size of the swollen particles for some studies have been larger than 100 nm[2, 3, 8-10]. Unfortunately, minimum size limitations are present when using conventional cross-linking polymerisation reactions[1] which has led to nanogels being prepared either using methods that provide either low yields or are not well-suited to scale-up such as coacervation of pre-formed polymers[4], solution self-assembly[1], or precipitation polymerisation[11, 12]. Hydrogel particles containing a high concentration of –COOH groups are potentially very useful because these groups have been shown to enable pH-triggered particle swelling at pH values near physiological pH[13-15] and they are well suited to a range of functionalisation reactions[16]. However, the previous work was limited to microgel particles which had swollen particle sizes that were much larger than 100 nm[14, 15]. We therefore sought to prepare pH-responsive polyacid nanogels using a scalable synthesis. In this communication it is shown that nanogels can be synthesised using a modification of the scalable nanolatex preparation recently introduced by Nunes and Asua[17].

Recently, Nunes and Asua[17] reported a theory-guided emulsion polymerisation method for preparing sub-100 nm (non-crosslinked) nanoparticles. They noted that by including a small proportion of methacrylic acid (MAA) the nanoparticle size decreased due to an increased surfactant parking area. Microgels (crosslinked polyacid particles that swell when the pH increases to above the polymer pK_a) are much larger than nanogels and have been prepared containing ~ 35 mol.% of MAA[13, 14]. We hypothesised that an increase in the MAA content to high levels (e.g., greater than 10 mol.%) would provide an increased parking area for the surfactant (sodium dodecyl sulfate, SDS) and enable preparation of pH-responsive nanogels using a high yield, scalable approach.

Polyacid microgel particles can be vinyl-functionalised and concentrated dispersions covalently-interlinked to form injectable pH-responsive macrogels, which were termed doubly crosslinked microgels (DX MGs)[15]. Those systems had potential application for restoring the mechanical properties of damaged soft tissue. However, those DX MG systems were relatively brittle compared to high performance double network hydrogels[18]. They were also relatively turbid which may limit their potential for imaging in vivo using fluoresence. We hypothesised that the use of smaller polyacid nanogel particles would provide lower turbidity macroscopic gels with improved ductility due to the higher nanogel surface area. These two aspects, together with the ability to functionalise the nanogels, are demonstrated in the present work using the new polyacid nanogels. We further demonstrate injectable nanogel-based macrogels with near-infrared (NIR) emission, which is a particularly sought after property for imaging in vivo[19].

For this study we prepared four nanogel systems to demonstrate the versatility of our approach. They were prepared using emulsion polymerisation (See Scheme 1). The methods and quantities used to prepare all systems as well as details concerning characterisation are given in the Experimental Section and Table S1 (ESI†). N-1, N-2 and N-3 comprised poly(methyl methacrylate-co-MAA-co-ethyleneglycol dimethacrylate) (poly(MMA-MAA-EGDMA)). The N-4 nanogel comprised poly(ethylacrylate-co-MAA-co-1,4-butanediol diacrylate) (PEA-MAA-BDDA). N-1 and N-4

[a] School of Materials, University of Manchester, Manchester, M13 9PL, U.K.
[b] Department of Chemistry, The University of Sheffield, Dainton Building, Brook Hill, Sheffield, South Yorkshire, S3 7HF, UK
[c] Centre for Tissue Injury and Repair, Institute for Inflammation and Repair, Faculty of Medical and Human Sciences, University of Manchester, Oxford Road, Manchester, M13 9PT, U.K
[d] NIHR Manchester Musculoskeletal Biomedical Research Unit, Manchester Academic Health Science Centre, Manchester, UK

† Electronic Supplementary Information (ESI) available: Experimental procedures, Potentiometric titration data, SEM images, rheology data, swelling measurements, biocompatibility data, UV-Vis and PL spectra, tabulated characterisation data.

were prepared containing the highest crosslinker concentrations (1.0 mol.%) in order to minimise nanogel swelling and enabled the effect of primary monomer type to be investigated. N-2 and N-3 were prepared using the lowest crosslinker contents (0.5 mol.%) and enabled the effect of MAA content to be probed. The as-prepared solids contents for the nanogels were in the range 5 - 18% (Table S1, ESI†) and were at least a factor of 4 greater than those reported for other pH-responsive nanogels[12].

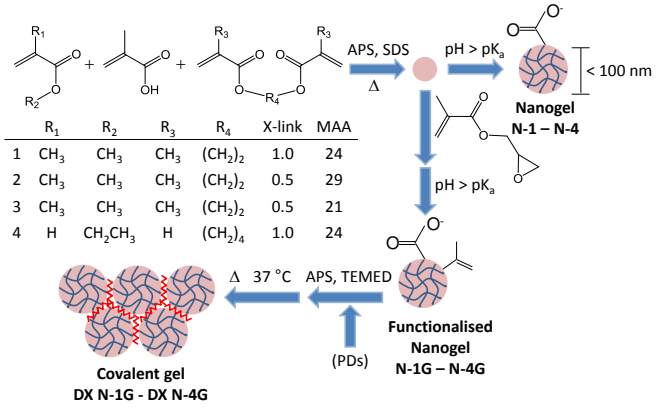

	R_1	R_2	R_3	R_4	X-link	MAA
1	CH_3	CH_3	CH_3	$(CH_2)_2$	1.0	24
2	CH_3	CH_3	CH_3	$(CH_2)_2$	0.5	29
3	CH_3	CH_3	CH_3	$(CH_2)_2$	0.5	21
4	H	CH_2CH_3	H	$(CH_2)_4$	1.0	24

Scheme 1. Depiction of the method used to prepare the pH-responsive nanogels (N-*x*), glycidyl methacrylate functionalised nanogels (N-*x*G) and macroscopic doubly crosslinked nanogels (DX N-*x*G). Polymer dots (PDs) were also mixed with N-*x*G to give fluorescent DX N-*x*G/PD composites. The nominal crosslinker and MAA concentrations shown are mol.%.

The MAA contents of N-1 to N-4 and apparent pK_a values were determined using potentiometric titration (Fig. S1, ESI†). The nanogels contained 20.4 to 29.2 mol.% **[N-2 needs to be repeated]** MAA and the apparent pK_a values were in the range 6.6 to 8.5 (Table S2, ESI†). The pK_a values for N-1, N-2 and N-4 were 7.3, 7.4 and 6.6, respectively. The latter values reside within the physiological pH range which is potentially important for future drug delivery applications. N-3 had the lowest measured MAA content (20.4 mol.%) and the highest pK_a which is the result of the greater hydrophobicity for this nanogel. The low pK_a for N-4 (of 6.6) is attributed to the greater flexibility of the poly(EA) chains. This general effect was reported earlier for linear poly(EA) and poly(MMA) copolymers containing MAA[20].

The nanogels were characterised by electronic microscopy (TEM or SEM). Fig. 1a shows the TEM for N-1 and TEM or SEM images are shown for the other systems in Fig. S2 (ESI†). The number-average diameters determined from electron microscopy were in the range of 17 – 51 nm (Table S2, ESI†). These values were comparable to the z-average diameter (d_z) values measured at pH ~ 6.0 which corresponds to the collapsed state of the nanoparticles (Table S2, ESI†). The nanogels were pH-responsive (Fig. 1b) and N-1, N-2 and N-4 swelled strongly as the pH approached their respective pK_a values. The N-3 system, which contained the lowest MAA content, showed the least pH-triggered swelling. The d_z values in the fully swollen state (pH ~ 9.0) were in the range of 44 to 58 nm and were well below 100 nm. Consequently, all four nanogels satisfied the size criteria for being termed nanogels.

The charge of the nanogels is an important feature because this affects dispersion stability and plays a crucial role in determining the interaction of particles with cells. The N-x dispersions were colloidally stable at pH values greater than ~ 5.5. The zeta potential as a function of pH was measured for N-1 and N-4 (see Fig. 1c) and shows that the particles were negatively charged. It is understood that zeta potential is not strictly correct for soft swollen gel particles[21]. However, we use this parameter because it provides a ball-park guide to the extent of electrostatic interactions present. The zeta potentials increased in magnitude with increasing pH due to the neutralisation of surface –COOH groups. The nanogel dispersions had excellent optical clarity (Fig. 1d). They were transparent whereas a comparable microgel dispersion was turbid. The improved transparency is due to the smaller particle size for the N-x particles.

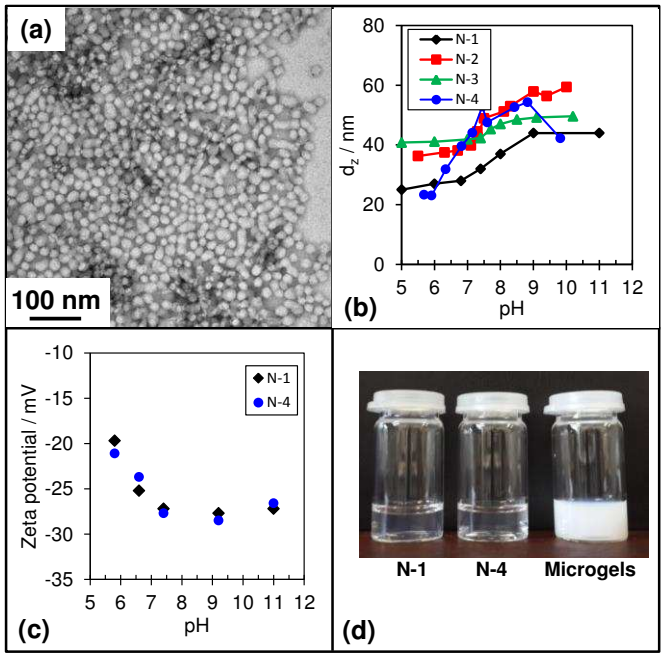

Figure 1. (a) TEM image of N-1. (b) DLS data as a function of pH for N-1 to N-4. (c) Zeta potential vs. pH data for N-1 and N-4. (d) Sample vials containing N-1 and N-4 and a microgel dispersion are shown. The particle concentration was 2.0 wt.% for N-1 and N-4 and the pH values were 5.6 and 5.5, respectively. The microgel dispersion concentration and pH were 2.0 wt.%, and 5.2 respectively.

It is well known that –COOH groups can act as chemical handles for a range of functionalisation chemistries[16]. Our nanogels were well suited to functionalisation whilst retaining their pH-responsive properties because of their high MAA contents. In order to demonstrate the ability to functionalise the nanogels they were reacted with glycidyl methacrylate (GMA) as shown in Scheme 1. The GMA contents were determined from potentiometric titration data (Fig. S3, ESI†) and were in the range of 2.5 to 4.4 mol.% (Table S2, ESI†). The pK_a values did not change greatly upon functionalisation for N-1G, N-2G and N-4G. Interestingly, the pK_a for N-3G moved closer to the physiological range. TEM (Fig. 2a and Fig. S4b, ESI†) and SEM data (Fig. S4a, ESI†) showed that the nanogel size and morphology and was not affected by functionalisation. Interestingly, the MMA-containing functionalised nanogels (N-1G, N-2G and N-4G) showed increased pH-responsiveness (Fig. 2b) which seems counter-intuitive at first site because they had lower MAA contents (Table S2, ESI†). This trend was most pronounced for N-2G which was prepared using the lowest crosslinker content and had a d_z value of 105 nm at pH 9. The increased swelling was due to plasticising of the poly(MMA) chains during the solvent washing process and was

reported for much larger microgel particles earlier[14]. The construction of nanogels using a higher crosslink content (N-1G) or lower MAA content (N-3G) enabled the swollen diameters of the functionalised nanogels to remain below 100 nm.

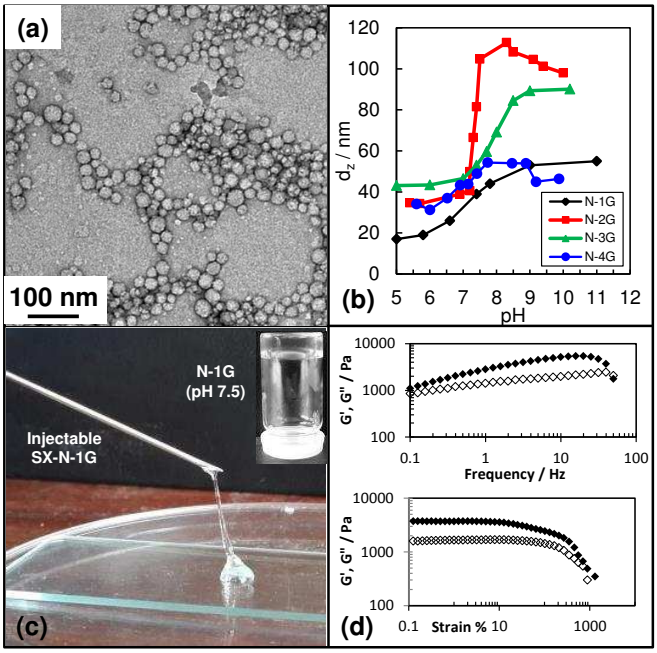

Figure 2. (a) TEM image of N-1G particles. (b) DLS data as a function of pH for N-*x*G (*x* = 1 – 4). (c) Images of concentrated dispersion N-1G (21 wt.%) and demonstration of injectability of N-1G dispersion (12 wt.%). (d) Frequency sweep (top) and strain sweep (bottom) rheology data for concentrated N-1G dispersions at pH 7.5. G' (shear modulus) and G" (storage modulus) are the closed and open symbols, respectively.

Because of the ability of the nanogels to swell with increasing pH concentrated dispersions had potential to form injectable viscous fluids and physical gels near physiological pH. N-1G dispersions containing a particle concentration of 12 wt. % were low viscosity fluids at pH 7.5 as shown by rheology data (Fig. S5, ESI†) and was injectable (Fig. 2c). The fluid could be transformed into elastomeric covalently interlinked linked hydrogels (below). When the N-1G concentration was increased to 21 wt.% the dispersion underwent a pH-triggered fluid-to-gel transition when the pH was increased to 7.5 and provided a self-supporting transparent physical gel (Fig. 2c). The latter was shear-thinning as shown by frequency-sweep and strain-sweep rheological data (Fig. 2d). The former data showed that the storage modulus (*G'*) decreased when the frequency (Fig. 2d) increased, as expected for a weak gel. The strain-sweep data (Fig. 2d) showed that *G'* approached the loss modulus (*G"*) at high strains, due gel breakdown.

To demonstrate the potential of functionalised nanogels we used concentrated N-1G dispersions (12 wt.%) to synthesise new covalently interlinked hydrogels (See Scheme 1). It was hypothesised that as the pH was increased the peripheries of the nanogels within would come into contact and enable covalent interlinking. Here, the nanogels would act as macro-crosslinkers. The covalent coupling of the vinyl groups introduced a second level of crosslinking in addition to the first intra-nanogel crosslinking from EGDMA. The hydrogels are termed doubly crosslinked (DX) nanogels. In contrast to the earlier DX microgels[14] we discovered that DX nanogels could be prepared from dispersions that were not physical gels, e.g., the low viscosity fluid shown in Fig. 2c. We speculate that the high surface area-to-volume ratio of nanogels enabled a higher concentration of covalent inter-nanogel linkages to form which enabled elastomeric gel formation from low viscosity fluids.

The DX N-G hydrogels were optically transparent (Fig 3a). Furthermore, they showed pH-triggered swelling (Fig. S6, ESI†). MTT assays for nucleus pulposus cells in the presence of DX N-1G indicated that the gels had no detectable cytotoxicity (Fig. S7, ESI†). The DX N-1G also had very low absorbance values as can be seen from the UV-visible spectrum for a disc with a thickness of 1.5 mm shown in Fig. 3b. The scattering from these DX N-1G hydrogels contrasts to the previous DX microgels which were turbid[14, 15]. The primary reason for the latter is the much smaller size of the nanogels.

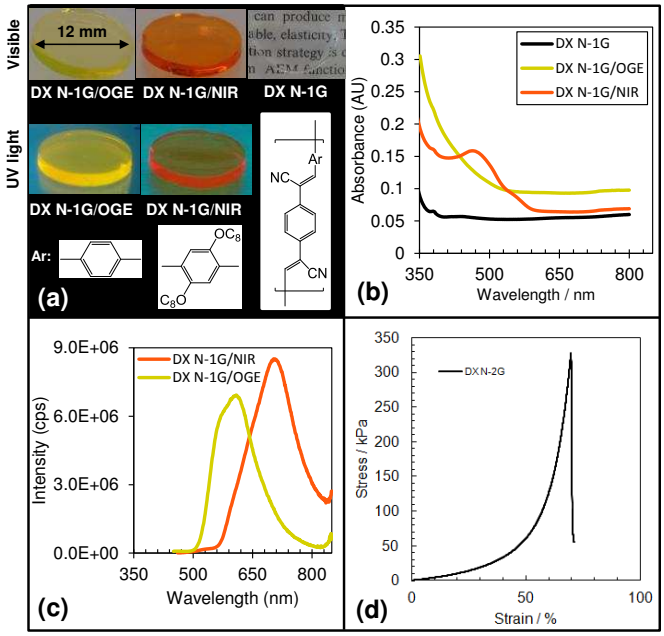

Figure 3. (a) Digital photographs of various DX N-1G hydrogel and DX N-1G/polymer dot (PD) composites obtained using visible and UV light (λ = 365 nm). (b) UV-visible spectra for DX N-1G gel and composites. (c) PL spectra for the DX N-1G/PD composites (λ_{ex} = **xxx** nm). (d) Stress-strain data for DX Nx-G hydrogels. **[Nam to provide value for λ_{ex}]**

There has been a strong interest in using conjugated polymer nanoparticles (CP NPs) for in vivo applications[22, 23]. We took advantage of the excellent optical clarity of the DX NGs to construct all-colloidal DX N-1G/CP NP hydrogel composites. Two CP NP dispersions were synthesised using a modification of the method of Kim et al.[22] (See ESI†) and the dispersions were blended with the N-1G particles prior to covalent DX N-1G/CP NP formation. The gels showed strong fluorescence when viewed under UV light (Fig. 3a). UV-visible spectra for the CP NPs, which were dispersed in water with a size ~ 50 nm, are shown in Fig. S8 (ESI†). The UV-visible spectra for the DX N-1G/CP NP composites showed a maximum for the NIR CP NPs and only a scattering shoulder for the OGE CP NPs. This behaviour is because the absorption maximum (λ_{max}) for the OGE PDs was ~ 325 nm (Fig. S8, ESI†) which corresponded to the scattering region from the PDs within the hydrogel. The λ_{max} value was slightly red-shifted from a value of 460 nm for the NIR dispersion (Fig. S8, ESI†) to a value of 464 nm within the hydrogel composite.

Photoluminescence (PL) spectra were measured (Fig. 3c) and were generally similar to those for the respective CP NPs (Fig. S9, ESI†). However, the spectrum for the DX N-1G/NIR system had an emission maximum at 705 nm and was red-shifted by ~ 30 nm compared to the parent CP NPs, which had an emission maximum at 670 nm. It is not certain at this stage why the red-shift occurred, although it was found to be reproducible. The shift did not occur for the OGE PDs. Such a shift is potentially beneficial because it brings the emission into the near-infrared region which is highly penetrating in tissue[19]. This raises the interesting possibility of using DX N-1G/NIR gels as an imaging gel within the body and this will be pursued in future work.

The mechanical properties of the DX N-xG hydrogels were investigated using uniaxial compression data (See Fig. 3d) because of their potential for their longer term use for the repair of damaged load-bearing tissue[14]. The values for the compression modulus (E), shear-at-break (σ_B) and strain-at-break (ε_B) are shown in Table S3 (ESI†). The E and ε_B values were 37 kPa and 70 %, respectively. **[More values coming]** Interestingly, the ε_B value is 40% higher compared to the value reported for a comparable DX microgel[24]. The E value is about half that for the DX microgel. These results show that the use of nanogels provides more ductile DX gels. Consequently, these DX nanogel systems should provide enhanced opportunity for load support within soft tissue where high ductility is required. **[Awaiting data for DX N-1G. If we can also obtain data for DX N-3G that will help. Take photos of these gels].**

In conclusion, this study reports a versatile scalable synthesis for pH-responsive nanogel particles with diameters less than 100 nm for the first time. Furthermore, we have demonstrated that the particles retained good swelling properties when functionalised with GMA. The functionalised nanogels formed injectable fluids and shear-thinning physical gels that were able to be transformed into transparent hydrogels under physiological conditions. The DX N-1G gels were not cytotoxic, had excellent mechanical properties and could be prepared as composites using CP NPs. Furthermore, the composite DX N/CP NP gels exhibited NIR fluorescence and may have potential for a dual load-supporting / remote imaging system in the future. Consequently, the new pH-responsive nanogels presented here for the first time have a great deal of potential to enable preparation of new families of functionalised nanogels and gels which may have use in a range of areas including as injectable imaging gels which provide load support in regions subject to high strain.

Acknowledgements

BRS and SPA would like to thank the EPSRC for funding this research (EP/K030949/1 & EP/K03071X/1). We also thank Annie Pallis for preparing and characterising one of the nanogels. BRS gratefully acknowledges a 5 year EPSRC Established Career Fellowship (M002020/1).

Notes and references

1. N. Morimoto, S. Hirano, H. Takahashi, S. Loethen, D. H. Thompson and K. Akiyoshi, *Biomacromolecules*, 2013, **14**, 56-63.
2. G. B. Demirel and R. von Klitzing, *ChemPhysChem*, 2013, **14**, 2833-2840.
3. H. A. Abd El-Rehim, A. E. Swilem, A. Klingner, E.-S. A. Hegazy and A. A. Hamed, *Biomacromolecules*, 2013, **14**, 688-698.
4. W.-H. Chiang, V. T. Ho, W.-C. Huang, Y.-F. Huang, C.-S. Chern and H.-C. Chiu, *Langmuir*, 2012, **28**, 15056-15064.
5. A.-C. Hellgren, P. Weissenborn and K. Holmberg, *Prog. Org. Coat.*, 1999, **35**, 79-87.
6. A. Aymonier, E. Papon, J. J. Villenave, P. Tordjeman, R. Pirri and P. Gérard, *Chem. Mater.*, 2001, **13**, 2562-2566.
7. L. Bromberg and L. Salvati, *Bioconjugate Chem.*, 1999, **10**, 678-686.
8. H. Hayashi, M. Iijima, K. Kataoka and Y. Nagasaki, *Macromolecules*, 2004, **37**, 5389-5396.
9. L. Lin, W. Xu, H. Liang, L. He, S. Liu, Y. Li, B. Li and Y. Chen, *Colloids Surf., B*, 2015, **126**, 459-466.
10. H. Urakami, J. Hentschel, K. Seetho, H. Zeng, K. Chawla and Z. Guan, *Biomacromolecules*, 2013, **14**, 3682-3688.
11. L.-W. Xia, R. Xie, X.-J. Ju, W. Wang, Q. Chen and L.-Y. Chu, *Nat Commun*, 2013, **4**.
12. X. Li, J. Zuo, Y. Guo and X. Yuan, *Macromolecules*, 2004, **37**, 10042-10046.
13. B. R. Saunders, N. Laajam, E. Daly, S. Teow, X. Hu and R. Stepto, *Adv. Colloid Interface Sci.*, 2009, **147–148**, 251-262.
14. R. Liu, A. H. Milani, T. J. Freemont and B. R. Saunders, *Soft Matter*, 2011, **7**, 4696-4704.
15. A. H. Milani, A. J. Freemont, J. A. Hoyland, D. J. Adlam and B. R. Saunders, *Biomacromolecules*, 2012, **13**, 2793-2801.
16. H. R. Culver, S. D. Steichen, M. Herrera-Alonso and N. A. Peppas, *Langmuir*, 2016, **32**, 5629-5636.
17. J. d. S. Nunes and J. M. Asua, *Langmuir*, 2012, **28**, 7333-7342.
18. J. P. Gong, *Soft Matter*, 2010, **6**, 2583-2590.
19. C. Zhu, L. Liu, Q. Yang, F. Lv and S. Wang, *Chem. Rev.*, 2012, **112**, 4687-4735.
20. R. Bird, T. Freemont and B. R. Saunders, *Soft Matter*, 2012, **8**, 1047-1057.
21. H. Ohshima, K. Makino, T. Kato, K. Fujimoto, T. Kondo and H. Kawaguchi, *J. Colloid Interface Sci.*, 1993, **159**, 512-514.
22. S. Kim, C.-K. Lim, J. Na, Y.-D. Lee, K. Kim, K. Choi, J. F. Leary and I. C. Kwon, *Chem. Commun.*, 2010, **46**, 1617-1619.
23. K. Li and B. Liu, *J. Mater. Chem.*, 2012, **22**, 1257-1264.
24. A. H. Milani, J. Bramhill, A. J. Freemont and B. R. Saunders, *Soft Matter*, 2015, **11**, 2586-2595.

